RNA Seeds Higher-Order Assembly of FUS Protein

Jacob C. Schwartz,[1] Xueyin Wang,[1] Elaine R. Podell,[1] and Thomas R. Cech[1,*]
[1]Howard Hughes Medical Institute, Department of Chemistry and Biochemistry, BioFrontiers Institute, University of Colorado, Boulder, CO 80309, USA
*Correspondence: thomas.cech@colorado.edu
http://dx.doi.org/10.1016/j.celrep.2013.11.017

SUMMARY

The abundant nuclear RNA binding protein FUS binds the C-terminal domain (CTD) of RNA polymerase II in an RNA-dependent manner, affecting Ser2 phosphorylation and transcription. Here, we examine the mechanism of this process and find that RNA binding nucleates the formation of higher-order FUS ribonucleoprotein assemblies that bind the CTD. Both the low-complexity domain and the arginine-glycine rich domain of FUS contribute to assembly. The assemblies appear fibrous by electron microscopy and have characteristics of β zipper structures. These results support the emerging view that the pathologic protein aggregation seen in neurodegenerative diseases such as amyotrophic lateral sclerosis may occur via the exaggeration of functionally important assemblies of RNA binding proteins.

INTRODUCTION

Eukaryotic cells have many examples of self-assembled bodies, which are concentrated protein structures not bound by lipid membranes. Examples in the cytoplasm include P bodies and stress granules (Decker and Parker, 2012). Nuclear assemblies include the nucleolus, Gemini of coiled bodies, Cajal bodies, histone locus bodies, promyelocytic leukemia bodies, paraspeckles, and splicing speckles (Nizami et al., 2010). These structures are rich in RNA binding proteins, and, in some cases, their assembly may be nucleated by RNA itself (Kaiser et al., 2008).

Some RNA binding proteins that comprise self-assembled structures contain a low-complexity (LC) domain, which, in isolation, has the ability to form amyloid-like structures (Sun et al., 2011; Han et al., 2012; Kato et al., 2012). One such protein is FUS, an abundant nuclear protein that affects multiple levels of RNA biogenesis, including transcription, splicing, and mRNA transport (Yang et al., 2000; Wang et al., 2008; Polymenidou et al., 2012). Mutations in FUS cause 5% of familial and rarely sporadic amyotrophic lateral sclerosis (ALS), a neurodegenerative disease leading to the death of motor neurons (Kwiatkowski et al., 2009; Vance et al., 2009; Polymenidou et al., 2012). At autopsy, large cytoplasmic aggregates stain positive for FUS in the motor neurons of ALS patients with these mutations.

In cells, FUS binds RNA polymerase II (RNAP2) and affects transcription (Yang et al., 2000; Das et al., 2007; Wang et al., 2008; Schwartz et al., 2012; Tan et al., 2012). The loss of FUS or overexpression of FUS leads to altered gene expression for thousands of genes in many different cell types (Hoell et al., 2011; Ishigaki et al., 2012; Lagier-Tourenne et al., 2012; Schwartz et al., 2012; Tan et al., 2012). In our previous work, we characterized FUS binding to RNAP2 through its C-terminal domain (CTD) (Schwartz et al., 2012). FUS binds RNAP2 at the transcription start sites of more than 50% of expressed genes in human embryonic kidney (HEK) 293T/17 cells and orchestrates Ser2 phosphorylation. Purified FUS binds the CTD in an RNA-dependent manner (Schwartz et al., 2012).

Here, we investigate the mechanism by which RNA potentiates the FUS-CTD interaction. We show that RNA stimulates the formation of higher-order FUS structures. We isolate two domains within FUS that contribute to higher-order assembly. Finally, the CTD of RNAP2 binds these FUS structures, suggesting a model for RNA-dependent recognition of the CTD by FUS.

RESULTS

Highly Cooperative Binding of FUS to Multiple RNA Sequences

Although previous studies identified RNA sequence and structure motifs that bind FUS (Lerga et al., 2001; Hoell et al., 2011; Ray et al., 2013), any comprehensive model of FUS function must account for the broad RNA binding seen in crosslink experiments followed by immunoprecipitation and sequencing (Schwartz et al., 2012). Therefore, we tested a 48 nt RNA from the promoter of gene DNMT3b; this prD RNA, one of many sequences identified previously (Schwartz et al., 2012), contains none of the published FUS binding motifs (Figure S1A). Purified, monomeric FUS (Figure S1B) bound this RNA with reasonably high affinity (K_d^{app} = 97 ± 2 nM) and high cooperativity (apparent Hill coefficient, n = 4.0 ± 0.2) (Figure 1A). Because n is the minimum number of interacting binding sites in a system showing positive cooperativity, the simplest conclusion is that at least four FUS proteins are bound to prD RNA in complex 3.

To assess whether some unidentified sequence or structure motif in prD RNA was responsible for its binding to FUS, we replaced either its 5′ or 3′ half with poly(A) (Figure 1B). These 48 nt RNAs bound FUS with affinities similar to that of the parental prD RNA, indicating that the stem-loop structure in the 5′ half of prD was not necessary for binding. Poly(A) itself weakly bound FUS (Figure 1B). Furthermore, three RNAs with abundant secondary
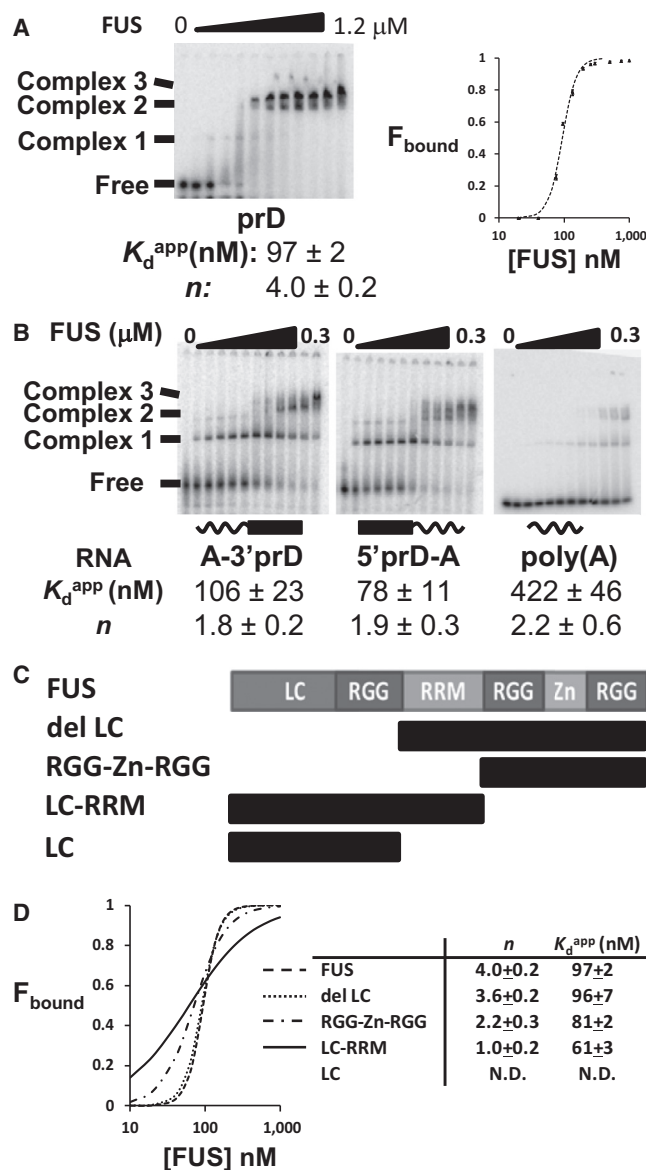
Figure 1. FUS Binds RNA in a Highly Cooperative, but Not Highly Sequence-Specific, Manner

(A) Left, trace prD RNA was incubated with increasing concentrations of full-length MBP-FUS protein (0 to 1,200 nM), and binding was analyzed by electrophoretic mobility shift assay (EMSA). Right, quantification of F_{bound} = RNA in complexes per total RNA in lane as a function of FUS concentration. Data were fit with a binding curve; Hill coefficient n = 4. Error bars (which are small) represent the range of data from two independent experiments.

(B) EMSA experiments for the RNA variants shown in Figure S1A, all binding to full-length FUS. Uncertainties listed for K_d^{app} and n represent the range of two or more replicates.

(C) Domain structure of FUS protein and truncated versions of the protein that were tested for RNA binding.

(D) Summary of prD RNA binding data for truncation mutants of FUS. Uncertainties represent the range of two or more replicates. The LC domain bound RNA so weakly that binding parameters were not determined (N.D.). Samples of primary data are shown in Figure S2.

structure—two group I intron domains (Bp P456 and Pne P456) and the medaka telomerase RNA (Med TR)—all bound FUS with moderate affinity (K_d^{app} = 46 to 111 nM) and high cooperativity (n = 3 to 4) (Figure S1B). GGUG RNA, containing a proposed FUS binding motif (Lerga et al., 2001), and its negative control CCUC RNA bound with lower affinity (Figure S1C). In conclusion, FUS binding is not highly specific for RNA sequence or structure.

The electrophoretic mobilities of the FUS-RNA complexes gave additional information. When poly(A) was substituted for either half of prD, binding was less cooperative (n = 1.7 to 2.0), and the intermediate complex 1 accumulated much more than with prD RNA (Figure 1B). This suggests that, when half of prD is attached to the weak-binding poly(A) sequence, the prD portion binds two FUS molecules cooperatively (complex 1), and FUS then binds the poly(A) segment to give complexes 2 and 3 only at high [FUS]. The observation of such discrete complexes indicates well-folded protein. We conclude that diverse RNA sequences can bind multiple FUS proteins in a highly cooperative manner.

Contributions of FUS Domains to RNA Binding

The FUS protein has an N-terminal LC domain capable of forming fibrous structures in isolation (Kato et al., 2012) followed by two RNA binding domains—an RNA recognition motif (RRM) and a zinc finger (Figure 1C). Arginine-glycine-rich (RGG) domains surround each RNA binding domain. Both the RRM-containing and zinc-finger-containing (RGG-Zn-RGG) domains bound prD RNA (Figure 1D), consistent with a previous study (Iko et al., 2004). The LC domain did not bind RNA (Figure S1D). We found that the binding affinities of the two domains were very similar to each other and to that of the full-length protein—this may indicate that only one RNA binding domain is available for binding in the full-length protein. Full binding cooperativity required both RNA binding and RGG domains (see full-length FUS and del-LC); RGG-Zn-RGG bound with intermediate cooperativity, and LC-RRM bound with full affinity but reduced or no cooperativity.

RNA Interactions Promote FUS Binding to the CTD of RNAP2

We investigated the RNA dependence of FUS binding to the CTD of RNAP2. Titration of the prD RNA showed that FUS pulled down with GST-CTD at a half-maximum RNA concentration similar to the K_d^{app} of this RNA for FUS (Figure 2A). Multiple RNAs with sequences from gene promoters bound by FUS in HEK 293T/17 cells, along with a variety of other noncoding RNAs, also promoted FUS pull-down with GST-CTD (Figure 2B). In multiple experiments, similar CTD binding occurred with maltose binding protein (MBP)-FUS containing an N-terminal MBP solubility tag, as with H6-FUS (data not shown). Not all RNAs were able to promote FUS-CTD binding. Nonhuman sequences, including the P456 domain of the *Tetrahymena* group I intron, were active. Interestingly, a point mutant in P456 disrupting the RNA tertiary structure abolished its ability to promote FUS to bind the CTD. Despite showing no activity in promoting FUS-CTD interaction, RNAs Bp P456, Pne P456, and Med TR had high affinity for FUS binding. Thus, it
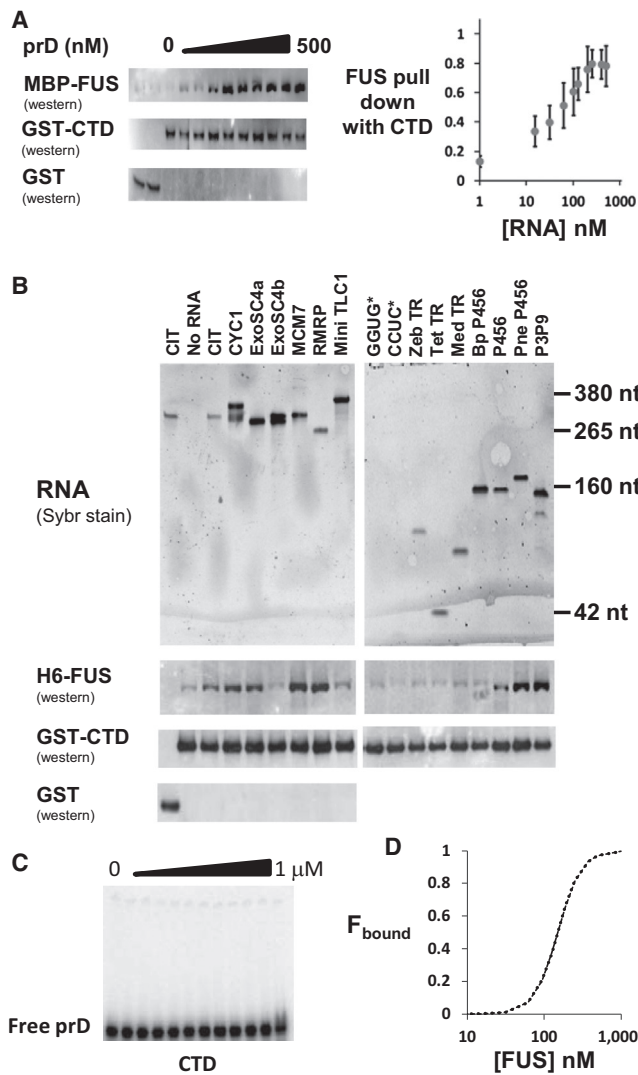
Figure 2. RNA Promotes FUS Binding to the CTD of RNAP2

(A) Left, a representative western blot from pull-down of MBP-FUS by GST-CTD stimulated by titrating in the prD RNA. Lanes 1 and 2 test GST with no RNA or with the highest RNA concentration, respectively. Right, MBP-FUS binding to GST-CTD as a function of prD RNA concentration averaged from three replicates (error bars represent SEM).

(B) The ability of various RNAs to promote FUS binding to the CTD, including sequences from FUS-regulated gene promoters (citron [CIT], CYC1, ExoSC4, and MCM7), RMRP, telomerase RNAs (yeast mini-TLC1, *Tetrahymena* [Tet TR], zebrafish [Zeb TR], or medaka [Med TR]) (Xie et al., 2008), and various group I intron domains from *Tetrahymena* (P456 with defined tertiary structure, Bp P456 with disrupted tertiary structure, and P3P9) or *Pneumocystis (carinii) jirovecii* (Pne P456). The CIT RNA did not promote FUS to bind GST alone (left lane). Sequences GGUG and CCUC (Lerga et al., 2001) were too small to visualize on this Sybr-stained gel.

(C) Binding curve of GST-CTD for the prD RNA shows that CTD does not bind RNA.

(D) EMSA of FUS for RNA with (dashed line) or without (dotted curve) the presence of 1 μM GST-CTD reveals no change in the K_d^{app} of FUS for RNA.

appears that some RNA sequence or structure may be necessary for FUS to bind the CTD at the low concentrations tested.

One simple model for the FUS-RNA-CTD interaction would involve the CTD binding directly to RNA (Kaneko and Manley, 2005), and the RNA then bridging FUS and CTD. However, the CTD itself showed no stable binding to prD RNA (Figure 2C). Alternatively, the CTD could simultaneously contact RNA and FUS; in which case, the CTD should lower the K_d of FUS for RNA. However, FUS-RNA binding curves were unchanged in the presence of CTD (Figures 2D and S2).
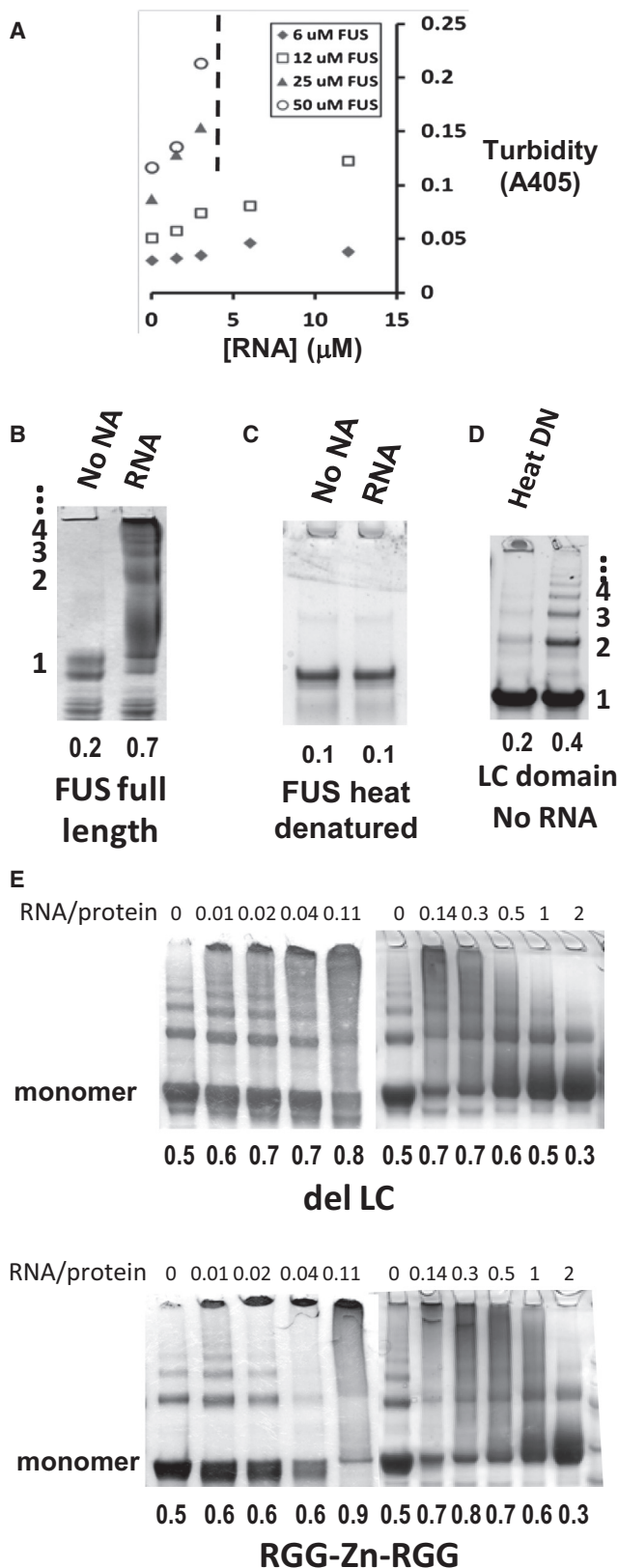
RNA Seeds FUS Assembly Formation

FUS has some ability to form higher-order assemblies without any RNA, especially at high concentrations (~100 μM) (Sun et al., 2011; Han et al., 2012; Kato et al., 2012). We found that assemblies were visible as an opalescent turbidity in solution, which could be quantified by measuring the absorbance at 405 nm. The addition of prD RNA promoted more assembly formation (Figure 3A). Low concentrations of FUS in the presence of RNA were able to form assemblies to the same extent as higher concentrations of FUS without RNA. High concentrations of FUS upon the addition of RNA eventually precipitated out of solution, preventing measurement (Figure 3A, vertical dashed line).

Using formaldehyde crosslinking, we found that the addition of prD RNA promoted FUS assembly with 70% of protein crosslinked in assemblies (Figure 3B). A distinct ladder consistent with up to five FUS proteins could be resolved by SDS-PAGE (Figure S3A). Single-stranded DNA with the same sequence as the prD RNA also promoted FUS assembly (Figure S3B). Furthermore, crosslinking FUS in the presence of RNA followed by nuclease treatment did not destroy the complexes, suggesting that they involve protein-protein crosslinks and not merely protein-RNA crosslinks (Figure S3C). No FUS crosslinking was observed when FUS was first heat denatured at 95°C, indicating that FUS structure is required for assembly (Figure 3C).

Formaldehyde crosslinking failed to detect LC domain assemblies. This is most likely due to the fact that LC contains no lysines. Therefore, we crosslinked LC assemblies with the use of UV irradiation. The amount of LC domain assemblies detected was reduced after heat denaturation of the protein (Figure 3D). This suggested that the LC domain possesses some structure required for assembly formation and that this assembly does not require RNA.

Next, we tested the RGG-Zn-RGG domain and the del-LC domain for their ability to assemble. Between 30% and 40% of del-LC and of RGG-Zn-RGG (Figures S3D and 3E) were crosslinked in higher-order assemblies without RNA, whereas 80% of the protein was in higher-order assemblies in the presence of the prD RNA or ssDNA. Other RNA sequences tested (Figure S1A) also promoted assembly formation to a degree consistent with their measured K_d^{app} (Figure 1B).

Substoichiometric levels of RNA promote assembly formation. RNA at concentrations 9- or 25-fold below that of the del-LC or RGG-Zn-RGG protein promoted the majority of the protein to form assemblies (Figure 3E, note Figure S3F for no crosslink control). At an RNA/protein ratio of 0.11, even with four FUS molecules bound to each RNA, more than half of the FUS in structures would be non-RNA-bound. Stoichiometric levels of RNA (the same concentration as the protein or higher) reduced assemblies to a level less than those seen in the absence of

Figure 3. RNA Seeds FUS Assembly

(A) FUS protein at various concentrations was incubated with or without RNA, and absorbance at 405 nm was measured (turbidity). Dashed line indicates that, at higher RNA concentrations, 25 and 50 μM FUS samples precipitated in a large opalescent gel, which prevented turbidity measurement.

(B) FUS incubated with or without 3 μM prD RNA in PBS (pH 6.0) and crosslinked with formaldehyde. Protein assemblies were resolved by SDS-PAGE and stained with Coomassie Blue.

(C) FUS was boiled at 95°C for 5 min and treated with formaldehyde as in (B).

(D) LC domain or heat-denatured LC (Heat DN) was crosslinked with UV and resolved by SDS-PAGE.

(E) The RNA binding domains del-LC and RGG-Zn-RGG (20 to 26 μM) were incubated with various concentrations of prD RNA and crosslinked with formaldehyde. Numbers below lanes indicate fraction of the total protein that was crosslinked.

RNA (Figure 3E). We performed the same experiments for full-length FUS and found a similar trend for RNA-dependent seeding and the inhibition of protein assembly at high [RNA] (Figure S3G).
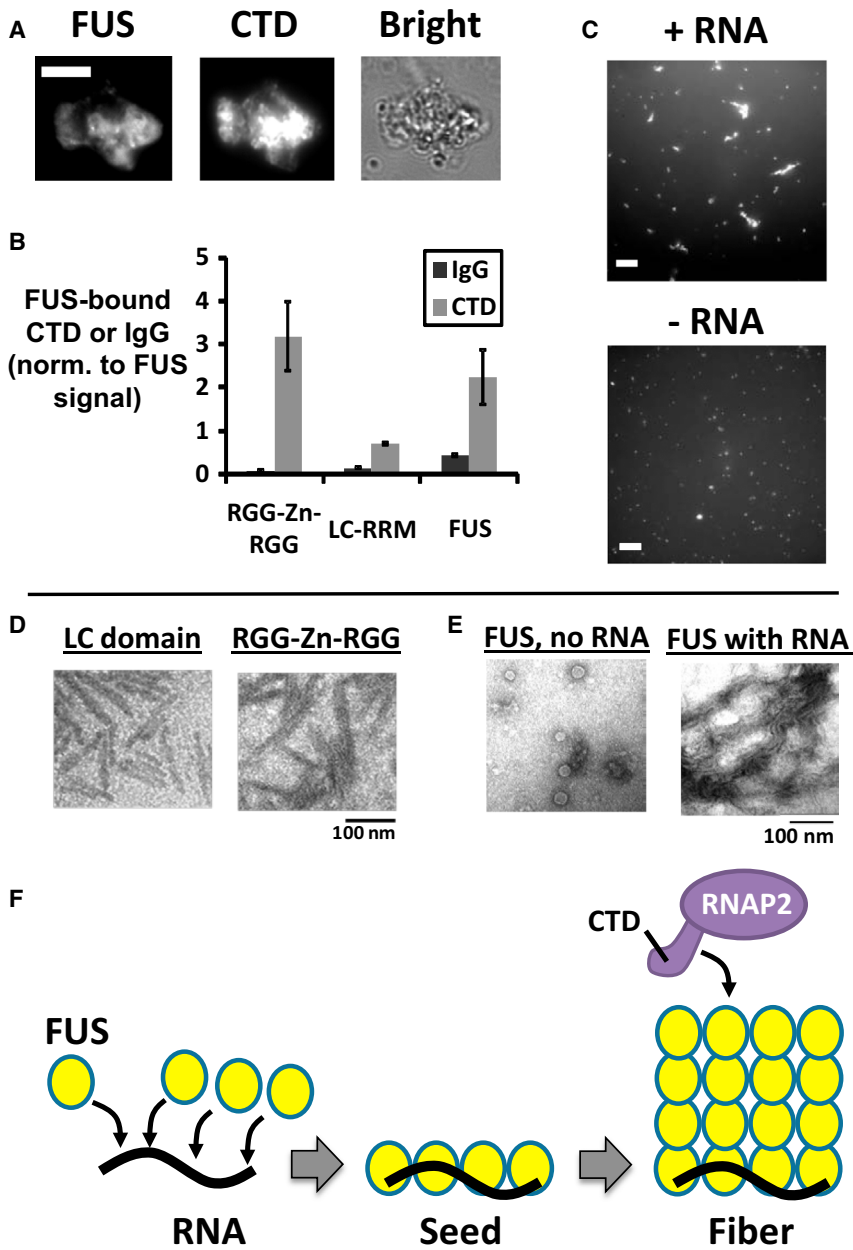
FUS Assemblies Bind the CTD of RNAP2

FUS assemblies were large enough to be visualized by light microscopy. Assemblies adhered to glass ranged from 1 to more than 5 μm across and appeared ropey (Figure S4A). In solution, they adopted a spherical shape consistent with phase transitions previously reported for protein hydrogels (Li et al., 2012) (Figure S4B). Protein constructs containing the assembly domains of FUS also readily formed microscopic hydrogels. These hydrogel assemblies weakly stained for the amyloid-specific fluorescent dye thioflavin T (ThT), suggesting the presence of some cross-β structure. ThT stains RNA, so all assemblies except LC stained brightly for ThT in the presence of RNA (Figure S4C). FUS is known to bind tightly to its own LC domain (Wang et al., 2008; Kato et al., 2012); therefore, we tested whether this domain would bind these FUS assemblies. We observed that LC remains stably associated with these assemblies after more than 48 hr incubation with fresh PBS (Figure S4D).

Then, we tested the ability of the CTD of RNAP2 to associate with these assemblies. FUS assemblies were allowed to form at high concentrations without the addition of RNA. GFP-CTD was incubated with the assemblies (Figure 4A). GFP-CTD remained bound to the FUS assemblies 2 days after fresh buffer exchange (Figure 4B, gray bars). Negative control protein (rabbit IgG) did not associate with FUS assemblies, even when it was monitored as early as 2 hr after changing the buffer (Figure 4B, black bars). Finally, LC-RRM and del-LC assemblies were incubated with GFP-CTD. After 48 hr, GFP signal was still detected above background. The signal normalized to FUS signal was higher for the del-LC construct than the LC-RRM (Figure 4B), suggesting that CTD associated more stably with the RGG-Zn-RGG domain of FUS.

The FUS assemblies in Figures 4A and 4B were formed without RNA in order to demonstrate that, once FUS assemblies are formed, they are capable of binding the CTD in the absence of RNA. However, in the presence of RNA, much larger FUS assemblies were formed that also bound GFP-CTD (Figure 4C).

A

FUS　　CTD　　Bright

B

FUS-bound CTD or IgG (norm. to FUS signal)

RGG-Zn-RGG　LC-RRM　FUS

C

+ RNA

- RNA

D

LC domain　　RGG-Zn-RGG

100 nm

E

FUS, no RNA　FUS with RNA

100 nm

F

FUS　RNA　Seed　Fiber　CTD　RNAP2

Figure 4. Assemblies of FUS Bind the CTD of RNAP2

(A) FUS assemblies were allowed to form at high concentration without RNA and spotted on glass cover slips. Assemblies were visualized by phase-contrast (Bright, right) and fluorescence microscopy (left). The scale bar represents 5 μm. FUS was visualized by immunofluorescence with anti-FUS. GFP-tagged CTD was incubated with FUS assemblies and remained bound up to 48 hr after incubation in PBS.

(B) After a 48 hr incubation, the signal from GFP-CTD or negative control AlexaFluor 633-conjugated rabbit IgG was measured and normalized by the signal for FUS, del-LC, or LC-RRM for each assembly (n > 30). Error bars represent SD.

(C) FUS (60 μM) assemblies were formed in the presence (top) or absence (bottom) of RNA (3 μM). Fluorescence indicates binding of GFP-CTD. The solid white scale bar represents 10 μm.

(D) MBP-tagged LC and RGG-Zn-RGG domains were stained with 1% uranyl acetate and imaged with TEM. LC and RGG-Zn-RGG both form polymeric fibers 70 to 150 nm long and either 30 (LC) or 10 nm (RGG-Zn-RGG) in diameter.

(E) Untagged FUS was incubated with or without prD RNA and imaged with TEM. Without RNA, most FUS appears in discs ranging from 30 to 50 nm in diameter. In most fields of view, large assemblies with a clear ropey subarchitecture are present.

(F) Model for RNA seeding of FUS assemblies. Multiple FUS proteins bind cooperatively along the RNA. The FUS-RNA complex forms a seed that organizes non-RNA-bound FUS into a fibrous assembly capable of binding the CTD of RNAP2.

ability to spontaneously form ropey assemblies but was mostly found in round, disk-shaped assemblies ranging from 30 to 50 nm in diameter. Upon the addition of RNA, large branched assemblies were formed, and subarchitecture that appeared as bundles of fibers forming the branches of these ropey structures could be observed (Figure 4E). We tested whether heat-denatured FUS could produce assemblies and did not observe any higher-order assemblies for denatured full-length FUS or LC-RRM.

We used circular dichroism spectroscopy to assess the secondary structure of FUS and domains of FUS. The domains LC-RRM and del-LC had spectra comprised almost entirely of β sheet and random coil (Figure S4E). The RGG-Zn-RGG domain remained soluble in a buffer (14 mM NaH₂PO₄ and 130 mM NaF) that allowed spectra to be collected for lower wavelengths (190 to 200 nm). This spectrum revealed RGG-Zn-RGG to be 49% β sheet and only 33% random coil. The LC domain was also largely β sheet (Figure S4E). These results support the conclusion that two domains of FUS, LC and RGG-Zn-RGG, form higher-order assemblies rich in β sheet structures.

FUS Forms Fibrous Assemblies in an RNA-Dependent Manner

We investigated the structure of FUS assemblies by transmission electron microscopy (TEM) after staining with uranyl acetate. Consistent with previous literature (Sun et al., 2011; Kato et al., 2012), the LC domain formed amyloid-like fibers approximately 30 in diameter and 50 to 100 nm long (Figure 4D). Interestingly, the RGG-Zn-RGG domain also formed fibrous assemblies approximately 10 to 15 nm wide and 100 nm or more long.

Full-length FUS was purified, the MBP tag was cleaved by PreScission protease, and assemblies were allowed to form by incubation at room temperature overnight by shaking. Upon investigation with TEM, FUS in the absence of RNA had some

DISCUSSION

RNA as a Regulator of FUS Assembly

Here, we show that FUS is triggered by binding RNA form higher-order assemblies. FUS assemblies utilize two domains common to proteins involved in cellular assemblies: the LC domain (Kato et al., 2012) and the RGG domain (this study). Each of these domains form fibrous assemblies largely comprised of β sheet secondary structure. In the absence of RNA binding, assembly requires very high protein concentrations. We find that FUS binds RNA with high cooperativity, implying the formation of a close-packed array of proteins on the RNA. We propose that this initial ribonucleoprotein (RNP) then nucleates assembly formation, allowing it to occur at protein concentrations that are physiologically relevant (Figure 4F). These assemblies function to selectively bind the CTD of RNAP2 and the LC domain of FUS. This suggests that FUS assemblies have the potential to affect transcription by forming a protein scaffold that recruits RNAP2. Kwon et al. (2013) have presented direct evidence that FUS assemblies can stimulate transcription in human cells and that this activity depends on the ability of FUS to form fibrous assemblies.

We find that RNA has the ability to both promote FUS assembly at low RNA/protein ratios and inhibit assembly at high RNA/protein ratios (Figure 3E). Such behavior is consistent with a model in which a FUS-RNA complex nucleates additional FUS proteins to be added. At high RNA ratios, all FUS is bound to RNA in nucleation complexes, and there are no free FUS proteins to polymerize. We find that FUS assemblies undergo significant structural reorganization upon binding to RNA. The full-length protein in the absence of RNA exists in disc-shaped assemblies. The size of these discs and the fact that their diameter varies (30 to 50 nm) suggests that multiple proteins comprise these structures. However, the molecules of FUS present in these assemblies are not in a structure that is efficiently crosslinked by formaldehyde.

Although the primary result of this paper is that RNA stimulates FUS assembly, an important question remaining is whether fibrous assemblies contribute to FUS-RNAP2 interactions in vivo. FUS affects RNAP2 recruitment, the efficiency of transcription, and the phosphorylation status on the CTD of RNAP2 (Yang et al., 2000; Schwartz et al., 2012, Kwon et al., 2013). An attractive model is that the efficiency of CTD recruitment to a FUS fibrous assembly would localize the polymerase to a greater extent than single FUS-CTD interactions. However, this model remains to be critically tested in vivo.

The RGG-Containing Domain of FUS Forms Fibers

Here, we show that the RGG-Zn-RGG domain unexpectedly forms fibrous assemblies in addition to those formed by the LC domain. RGG motifs are frequently found in RNA binding proteins and are well known to bind RNA (Thandapani et al., 2013). However, one study has suggested that the majority of RNA binding for FUS in vivo may be through the RRM (Daigle et al., 2013).

There is precedence for the implication of RGG motifs in the formation of protein assemblies. The RGG domain at the C terminus of nucleolin has been shown to mediate protein interactions

(Bacharach et al., 2000). The formation of translation-repressive mRNPs is regulated by RGG domains present in certain proteins that form assemblies with eiF4E and eiF4G (Rajyaguru et al., 2012). The first RGG domain in RGG-Zn-RGG of FUS has been predicted to be prion like (King et al., 2012). We find the domain RGG-Zn-RGG to have an unexpectedly high content of β strand secondary structure. Furthermore, we note that the crystal structure of an antifreeze protein of the snow flea, which possesses a highly similar amino acid motif XGG, reveals an unusual β sandwich structure stabilized by backbone hydrogen bonding rather than a more traditional hydrophobic core (Pentelute et al., 2008).

Implications of FUS Assemblies in Neurological Disease

Although higher-order polymer assemblies formed by proteins are fundamental to cellular function, higher-order assemblies can also contribute to disease pathology. The principles of RNA-promoted FUS assembly may apply more generally to the assembly of other RNA-rich bodies in the cell. Prion or LC domains contained in RNA binding proteins have been proposed to drive RNP granule assembly (Gilks et al., 2004; Decker et al., 2007). Likely candidates that may have similar propensity for RNA-promoted assembly include (1) those that have high sequence similarity (i.e., EWSR1 and TAF15), (2) those with related domain architectures (i.e., CIRBP and hnRNP proteins such as A1, A2B1, U, and A0), and (3) RGG-domain-containing proteins (i.e., FXRP1, nucleolin, LSM4, and fibrillin). An emerging theme is that the perturbation of the biologically important assembly of these RNA binding proteins can be pathogenic (Bosco et al., 2010; Ju et al., 2011; Kim et al., 2013; Ramaswami et al., 2013).

EXPERIMENTAL PROCEDURES

Protein Purification

Recombinant MBP-FUS or H6-FUS was expressed in and purified from BL21 *E. coli.* In brief, cells were lysed by sonication in lysis buffer (1 M KCl, 50 mM Tris [pH 7.4], 10 mM imidazole, 5% glycerol, 1% NP40, and 1.5 mM β-mercaptoethanol either with or without 1 M urea). Protein was extracted from the supernatant with Ni-Sepharose beads. Beads were washed four times in wash buffer (1 M KCl, 50 mM Tris [pH 7.4], 10 mM imidazole, and 1.5 mM β-mercaptoethanol either with or without 1 M urea). Protein was eluted in either wash buffer supplemented with 250 mM imidazole or PBS supplemented with 250 mM imidazole. See the Supplemental Experimental Procedures for details.

FUS-RNA Binding Curves

In a 20 μl reaction, a trace amount of [5′ ^{32}P] prD RNA was incubated with MBP-FUS in binding buffer (50 mM Tris-HCl [pH 7.4], 150 mM KCl, 2 mM MgCl$_2$, 2 mM dithiothreitol [DTT], 0.1 mg/ml yeast tRNA, 0.1 mg/ml BSA, and trace amount of orange dye) at room temperature for 30 min. 10 μl of each reaction was loaded onto a 4% to 20% Tris/borate/EDTA buffer (Invitrogen) gel and separated at room temperature at 150 V for 1.5 hr. The ^{32}P signal was detected with phosphorimager screens and quantified with ImageG. Curves and binding constants were calculated with MATLAB. MBP-FUS was pretreated with micrococcal nuclease in order to remove any nucleic acid that might have copurified.

CTD Pull-Down Assays

FUS (0 to 4 μM) and GST-CTD (0 to 1 μM) were incubated with different concentrations of prD RNA in 35 μl reaction buffer (50 mM Tris-HCl [pH 7.4], 150 mM KCl, 2 mM MgCl$_2$, 2 mM DTT, 0.1 mg/ml BSA, and 0.1 mg/ml yeast tRNA) for 30 min at room temperature. Complexes were immobilized with Glutathione Sepharose 4B beads (GE Healthcare). After washing, proteins

were eluted with 35 μl elution buffer (reaction buffer without BSA and yeast tRNA but containing 30 mM glutathione [pH 7.4] by KOH). Proteins were resolved on a 4% to 20% NuPAGE Bis-Tris Gel (Invitrogen),followed by western blotting with either anti-FUS (4H11, Santa Cruz Biotechnology) or anti-GST (ab3416, Abcam).

For more description, please refer to the Supplemental Experimental Procedures.

SUPPLEMENTAL INFORMATION

Supplemental Information includes Supplemental Experimental Procedures and four figures and can be found with this article online at http://dx.doi.org/10.1016/j.celrep.2013.11.017.

ACKNOWLEDGMENTS

REFERENCES

Bacharach, E., Gonsky, J., Alin, K., Orlova, M., and Goff, S.P. (2000). The carboxy-terminal fragment of nucleolin interacts with the nucleocapsid domain of retroviral gag proteins and inhibits virion assembly. J. Virol. 74, 11027–11039.

Bosco, D.A., Lemay, N., Ko, H.K., Zhou, H., Burke, C., Kwiatkowski, T.J., Jr., Sapp, P., McKenna-Yasek, D., Brown, R.H., Jr., and Hayward, L.J. (2010). Mutant FUS proteins that cause amyotrophic lateral sclerosis incorporate into stress granules. Hum. Mol. Genet. 19, 4160–4175.

Daigle, J.G., Lanson, N.A., Jr., Smith, R.B., Casci, I., Maltare, A., Monaghan, J., Nichols, C.D., Kryndushkin, D., Shewmaker, F., and Pandey, U.B. (2013). RNA-binding ability of FUS regulates neurodegeneration, cytoplasmic mislocalization and incorporation into stress granules associated with FUS carrying ALS-linked mutations. Hum. Mol. Genet. 22, 1193–1205.

Das, R., Yu, J., Zhang, Z., Gygi, M.P., Krainer, A.R., Gygi, S.P., and Reed, R. (2007). SR proteins function in coupling RNAP II transcription to pre-mRNA splicing. Mol. Cell 26, 867–881.

Decker, C.J., and Parker, R. (2012). P-bodies and stress granules: possible roles in the control of translation and mRNA degradation. Cold Spring Harb. Perspect. Biol. 4, a012286.

Decker, C.J., Teixeira, D., and Parker, R. (2007). Edc3p and a glutamine/asparagine-rich domain of Lsm4p function in processing body assembly in Saccharomyces cerevisiae. J. Cell Biol. 179, 437–449.

Gilks, N., Kedersha, N., Ayodele, M., Shen, L., Stoecklin, G., Dember, L.M., and Anderson, P. (2004). Stress granule assembly is mediated by prion-like aggregation of TIA-1. Mol. Biol. Cell 15, 5383–5398.

Han, T.W., Kato, M., Xie, S., Wu, L.C., Mirzaei, H., Pei, J., Chen, M., Xie, Y., Allen, J., Xiao, G., and McKnight, S.L. (2012). Cell-free formation of RNA granules: bound RNAs identify features and components of cellular assemblies. Cell 149, 768–779.

Hoell, J.I., Larsson, E., Runge, S., Nusbaum, J.D., Duggimpudi, S., Farazi, T.A., Hafner, M., Borkhardt, A., Sander, C., and Tuschl, T. (2011). RNA targets of wild-type and mutant FET family proteins. Nat. Struct. Mol. Biol. 18, 1428–1431.

Iko, Y., Kodama, T.S., Kasai, N., Oyama, T., Morita, E.H., Muto, T., Okumura, M., Fujii, R., Takumi, T., Tate, S., and Morikawa, K. (2004). Domain architec-

tures and characterization of an RNA-binding protein, TLS. J. Biol. Chem. 279, 44834–44840.

Ishigaki, S., Masuda, A., Fujioka, Y., Iguchi, Y., Katsuno, M., Shibata, A., Urano, F., Sobue, G., and Ohno, K. (2012). Position-dependent FUS-RNA interactions regulate alternative splicing events and transcriptions. Sci Rep 2, 529.

Ju, S., Tardiff, D.F., Han, H., Divya, K., Zhong, Q., Maquat, L.E., Bosco, D.A., Hayward, L.J., Brown, R.H., Jr., Lindquist, S., et al. (2011). A yeast model of FUS/TLS-dependent cytotoxicity. PLoS Biol. 9, e1001052.

Kaiser, T.E., Intine, R.V., and Dundr, M. (2008). De novo formation of a subnuclear body. Science 322, 1713–1717.

Kaneko, S., and Manley, J.L. (2005). The mammalian RNA polymerase II C-terminal domain interacts with RNA to suppress transcription-coupled 3′ end formation. Mol. Cell 20, 91–103.

Kato, M., Han, T.W., Xie, S., Shi, K., Du, X., Wu, L.C., Mirzaei, H., Goldsmith, E.J., Longgood, J., Pei, J., et al. (2012). Cell-free formation of RNA granules: low complexity sequence domains form dynamic fibers within hydrogels. Cell 149, 753–767.

Kim, H.J., Kim, N.C., Wang, Y.D., Scarborough, E.A., Moore, J., Diaz, Z., MacLea, K.S., Freibaum, B., Li, S., Molliex, A., et al. (2013). Mutations in prion-like domains in hnRNPA2B1 and hnRNPA1 cause multisystem proteinopathy and ALS. Nature 495, 467–473.

King, O.D., Gitler, A.D., and Shorter, J. (2012). The tip of the iceberg: RNA-binding proteins with prion-like domains in neurodegenerative disease. Brain Res. 1462, 61–80.

Kwiatkowski, T.J., Jr., Bosco, D.A., Leclerc, A.L., Tamrazian, E., Vanderburg, C.R., Russ, C., Davis, A., Gilchrist, J., Kasarskis, E.J., Munsat, T., et al. (2009). Mutations in the FUS/TLS gene on chromosome 16 cause familial amyotrophic lateral sclerosis. Science 323, 1205–1208.

Kwon, I., Kato, M., Xiang, S., Wu, L., Theodoropoulos, P., Mirzaei, H., Han, T., Xie, S., Corden, J.L., and McKnight, S.L. (2013). Phosphorylation-regulated binding of Rna polymerase ii to fibrous polymers of low-complexity domains. Cell 155, 1049–1060.

Lagier-Tourenne, C., Polymenidou, M., Hutt, K.R., Vu, A.Q., Baughn, M., Huelga, S.C., Clutario, K.M., Ling, S.C., Liang, T.Y., Mazur, C., et al. (2012). Divergent roles of ALS-linked proteins FUS/TLS and TDP-43 intersect in processing long pre-mRNAs. Nat. Neurosci. 15, 1488–1497.

Lerga, A., Hallier, M., Delva, L., Orvain, C., Gallais, I., Marie, J., and Moreau-Gachelin, F. (2001). Identification of an RNA binding specificity for the potential splicing factor TLS. J. Biol. Chem. 276, 6807–6816.

Li, P., Banjade, S., Cheng, H.C., Kim, S., Chen, B., Guo, L., Llaguno, M., Hollingsworth, J.V., King, D.S., Banani, S.F., et al. (2012). Phase transitions in the assembly of multivalent signalling proteins. Nature 483, 336–340.

Nizami, Z., Deryusheva, S., and Gall, J.G. (2010). The Cajal body and histone locus body. Cold Spring Harb. Perspect. Biol. 2, a000653.

Pentelute, B.L., Gates, Z.P., Tereshko, V., Dashnau, J.L., Vanderkooi, J.M., Kossiakoff, A.A., and Kent, S.B. (2008). X-ray structure of snow flea antifreeze protein determined by racemic crystallization of synthetic protein enantiomers. J. Am. Chem. Soc. 130, 9695–9701.

Polymenidou, M., Lagier-Tourenne, C., Hutt, K.R., Bennett, C.F., Cleveland, D.W., and Yeo, G.W. (2012). Misregulated RNA processing in amyotrophic lateral sclerosis. Brain Res. 1462, 3–15.

Rajyaguru, P., She, M., and Parker, R. (2012). Scd6 targets eIF4G to repress translation: RGG motif proteins as a class of eIF4G-binding proteins. Mol. Cell 45, 244–254.

Ramaswami, M., Taylor, J.P., and Parker, R. (2013). Altered ribostasis: RNA-protein granules in degenerative disorders. Cell 154, 727–736.

Ray, D., Kazan, H., Cook, K.B., Weirauch, M.T., Najafabadi, H.S., Li, X., Gueroussov, S., Albu, M., Zheng, H., Yang, A., et al. (2013). A compendium of RNA-binding motifs for decoding gene regulation. Nature 499, 172–177.

Schwartz, J.C., Ebmeier, C.C., Podell, E.R., Heimiller, J., Taatjes, D.J., and Cech, T.R. (2012). FUS binds the CTD of RNA polymerase II and regulates its phosphorylation at Ser2. Genes Dev. 26, 2690–2695.

Sun, Z., Diaz, Z., Fang, X., Hart, M.P., Chesi, A., Shorter, J., and Gitler, A.D. (2011). Molecular determinants and genetic modifiers of aggregation and toxicity for the ALS disease protein FUS/TLS. PLoS Biol. 9, e1000614.

Tan, A.Y., Riley, T.R., Coady, T., Bussemaker, H.J., and Manley, J.L. (2012). TLS/FUS (translocated in liposarcoma/fused in sarcoma) regulates target gene transcription via single-stranded DNA response elements. Proc. Natl. Acad. Sci. USA 109, 6030–6035.

Thandapani, P., O'Connor, T.R., Bailey, T.L., and Richard, S. (2013). Defining the RGG/RG motif. Mol. Cell 50, 613–623.

Vance, C., Rogelj, B., Hortobágyi, T., De Vos, K.J., Nishimura, A.L., Sreed- haran, J., Hu, X., Smith, B., Ruddy, D., Wright, P., et al. (2009). Mutations in FUS, an RNA processing protein, cause familial amyotrophic lateral sclerosis type 6. Science 323, 1208–1211.

Wang, X., Arai, S., Song, X., Reichart, D., Du, K., Pascual, G., Tempst, P., Rosenfeld, M.G., Glass, C.K., and Kurokawa, R. (2008). Induced ncRNAs allo- sterically modify RNA-binding proteins in cis to inhibit transcription. Nature 454, 126–130.

Xie, M., Mosig, A., Qi, X., Li, Y., Stadler, P.F., and Chen, J.J. (2008). Structure and function of the smallest vertebrate telomerase RNA from teleost fish. J. Biol. Chem. 283, 2049–2059.

Yang, L., Embree, L.J., and Hickstein, D.D. (2000). TLS-ERG leukemia fusion protein inhibits RNA splicing mediated by serine-arginine proteins. Mol. Cell. Biol. 20, 3345–3354.